

Variation in optical, dielectric and sintering behavior of nanocrystalline $\text{NdBa}_2\text{NbO}_6$

Kumpamthanath Chacko Mathai¹, Sukumariamamma Vidya², Sam Solomon³ and Jijimon Kumpukattu Thomas^{*2}

¹Department of Physics, St. Aloysius' College, Edathua-689573, Kerala, India

²Electronic Materials Research Laboratory, Department of Physics, Mar Ivanios College, Thiruvananthapuram- 695 015, Kerala, India

³Department of Physics, St. John's College, Anchal, Kollam District 691306, Kerala, India

(Received April 18, 2012, Revised March 21, 2013, Accepted March 29, 2013)

Abstract. High quality nanoparticles of neodymium barium niobium ($\text{NdBa}_2\text{NbO}_6$) perovskites have been synthesized using an auto ignition combustion technique for the first time. The nanoparticles thus obtained have been characterized by powder X-ray diffraction, thermo gravimetric analysis, differential thermal analysis, Fourier transform infrared spectroscopy, Raman spectroscopy and transmission electron microscopy. UV- Visible absorption and photoluminescence spectra of the samples are also recorded. The structural analysis shows that the nano powder is phase pure with the average particle size of 35 nm. The band gap determined for $\text{NdBa}_2\text{NbO}_6$ is 3.9 eV which corresponds to UV-radiation for optical inter band transition with a wavelength of 370nm. The nanopowder could be sintered to 96% of the theoretical density at 1325°C for 2h. The ultrafine cuboidal nature of nanopowders with fewer degree of agglomeration improved the sinterability for compactness at relatively lower temperature and time. During the sintering process the wide band gap semiconducting behavior diminishes and the material turns to a high permittivity dielectric. The microstructure of the sintered surface was examined using scanning electron microscopy. The striking value of dielectric constant $\epsilon_r = 43$, loss factor $\tan \delta = 1.97 \times 10^{-4}$ and the observed band gap value make it suitable for many dielectric devices.

Keywords: nanoparticles; combustion synthesis; perovskites; neodymium; barium niobate; sintering

1. Introduction

Luminescence in bulk solids showing wide band gap has been extensively studied for a long time (Aven and Prener 1967, Goldberg 1966). However nano crystals of such materials have acquired tremendous research interest in the recent past. Materials of wide band gap semiconductors are ideal for their studies of discrete states in the gap. Visible luminescence originates from transitions involving these localized states in the gap (Denzler *et al.* 1998). Wide band gap semiconductors have broad range of applications including light emitting devices, varistors, solar cells and gas sensors (Huang *et al.* 2001, Mahan 1983, Keis *et al.* 2002, Gruber *et al.* 2003). Perovskite oxides such as alkaline niobate crystal possess many interesting properties

*Corresponding author, Professor, E-mail: jkthomasemrl@yahoo.com

including piezoelectricity, pyroelectricity, electro-optic and nonlinear optical response (Bhalla *et al.* 2000). Its properties are also widely exploited in electronic devices particularly in telecommunication applications (Wooten *et al.* 2000). Niobium based intermetallic composites are recognized as an excellent source for future superconducting multi-filamentary conductors capable of operation even at magnetic fields much higher than 25 Tesla and under extreme mechanical and irradiation conditions (Specking *et al.* 1993). Koshy *et al.* synthesized niobium based double perovskite materials having good dielectric properties through solid state method; which are used as substrate for YBCO superconductors (Koshy *et al.* 1994, Jose *et al.* 2000).

In the miniaturization of cellular telephones, materials with dielectric constant greater than 40 are advisable. Cruickshank suggested that, for microwave dielectrics, it is possible to specify some minimum requirements such as the dielectric constant must lie between 35 and 55 for microwave dielectric device applications (Cruickshank 2003). The attractive dielectric properties ($\epsilon_r = 35-55$) directed the filter designers to use complex tantalates because of their higher selectivity and optimizing bandwidth (Hughes *et al.* 2001). The high demand for tantalum based filters increased their price and redirected the studies to a new composition based on isostructural niobium compounds (Dias 2006).

Complex Ba_2RENbO_6 (RE = Rare Earth elements) perovskite related ceramics synthesized through conventional solid state route have been studied by many researchers due to their tremendous applications in electronic materials research and industry (Koshy *et al.* 1993, Kurian *et al.* 1998). Among single perovskites, the most common alkaline niobate materials reported is lithium niobate ($LiNbO_3$). Since the discovery of ferroelectricity in $LiNbO_3$ (Matthias and Remeika 1949), its properties are widely exploited in electronic devices, particularly in telecom applications where the devices are fabricated from bulk or thin films material and serves as sensors, actuators, detectors or filters (Wooten *et al.* 2000). Potassium niobate ($KNbO_3$) is widely known for its large nonlinear coefficients ideal for wavelength conversion like second-harmonic generation (SHG), sum frequency mixing, as material in optical parametric oscillator or lead-free piezoceramics (Saito *et al.* 2004). Sodium niobate ($NaNbO_3$), however less studied on comparing $LiNbO_3$ and $KNbO_3$, also belongs to the alkaline niobates family. Generally, associated with potassium, $NaNbO_3$ is a very promising lead-free piezoelectric ceramics (Guo *et al.* 2004). Most of the work referred above deal with the synthesis of niobium-based perovskites, using conventional solid-state reaction method where the particles obtained are of many micron sizes.

Besides bulk and thin films structures, zero- (0D) and one-dimensional (1D) alkaline niobates nanostructures were also synthesized recently to combine the dimensional confinement with the other known properties of perovskite materials. The synthesis of nanostructured materials has generated great excitement and expectations in the past few years. Because of the extremely small dimensions, a large fraction of atoms in these materials are located at grain boundaries or surfaces interfacial components, lead to outstanding characteristics, that the bulk coarse-grained materials do not possess (Gleiter 2000). The major advantages of nanocrystalline materials are their superior phase homogeneity, hardness and strength, better sinterability and improved microstructures leading to excellent mechanical, electrical, dielectric, magnetic, optical and catalytic properties. Recent report on the preparation of nanopowders with superior features is one of the major research activities in materials processing technology (Suryanarayana 1994, Ramanujan 2003, Wang *et al.* 2005). The coarse-grained powders synthesized using the conventional solid-state route have the short coming of larger particle size yield, very high and prolonged processing temperatures and relatively poor class of purity.

Various synthesis routes have also been explored to obtain 0D nanoparticles or nanoflakes from

alkaline niobates such as mechano-chemical milling (Kong *et al.* 2008, Schwesyg *et al.* 2007), non-aqueous route (Niederberger *et al.* 2004), sol-gel method (Wang *et al.* 2007) or hydrothermal route (An *et al.* 2002), methods such as template assisted pyrolysis resulting in regular arrays of tubes (Zhao *et al.* 2005), solution-phase synthesis resulting in rod-like structures (Wood *et al.* 2008) or hydrothermal route giving free-standing nanowires with high aspect ratio (Magrez *et al.* 2006). However there are only few reports in literature on the synthesis of perovskites such as BaNbO_3 , SrNbO_3 and other alkaline earth niobates, on considering its tremendous applications.

Among the various techniques, solution synthesis offers improved phase homogeneity than the conventional solid state ceramic route. Patro *et al.* reported a combustion synthesis of strontium barium niobate in which a phase pure compound (SBN50) was obtained only after annealing at an elevated temperature of 700°C (Patro *et al.* 2003). Combustion synthesis technique also offers an easy and cost effective method for the synthesis of nanostructured materials (Aruna and Mukasyan 2008). Different approaches of combustion synthesis using varied chemicals as fuel, oxidizers and complexing agents were also reported (Chinarro *et al.* 2007, Deganello *et al.* 2009, Ianoş 2009). In all the combustion synthesis techniques reported, require a post calcination of the precursors after combustion, for the formation of pure phase. Recently a new technique in which a modified combustion synthesis and auto igniting, employing citric acid as complexing agent and ammonia as fuel was reported for the synthesis of nanomaterials (James 2004). This method requires no calcination step since phase pure materials are obtained directly after combustion. In some of our earlier communications we have also reported the modified auto igniting combustion synthesis of ABO_3 perovskites based on Zirconates, Halfnates etc. which shows improved powder characteristics as well as good sinterability with a substantial reduction in the sintering temperature to $\sim 200^\circ\text{C}$ and a lowered sintering time to ~ 3 hours (Padmakumar *et al.* 2008, Thomas *et al.* 2006, Prasanth *et al.* 2008). This may be due to the varying particle size and morphology of the nanomaterials prepared by the combustion technique (Zupan *et al.* 2004). A drastic change in properties particularly the optical behavior between nano powders and their sintered pellets were also observed in all the samples (Henglein 1989). In the present work, we report variation in optical, dielectric and sintering behavior of nanocrystalline $\text{NdBa}_2\text{NbO}_6$ perovskites synthesized, through the auto-ignition combustion technique.

2. Experimental details

All the reagents and solvents used in the combustion synthesis of nanopowders of $\text{NdBa}_2\text{NbO}_6$ were of analytical grade and were directly used without any further purification process.

2.1 Preparation

In the modified single step auto-ignition combustion synthesis, an aqueous solution containing Nb^{5+} was prepared by dissolving typical amount of high purity NbCl_5 (Alpha Aesar 99.9%) in hot oxalic acid solution in a glass beaker. Aqueous solution containing ions of Ba and Nd were prepared by dissolving stoichiometric amount of high purity $\text{Ba}(\text{NO}_3)_2$ (99% CDH, India) in double distilled water and Nd_2O_3 (99% CDH, India) in dilute HNO_3 . Citric acid was then added as complexing agent and urea as the fuel to the solution containing stoichiometric amount of Ba, Nd and Nb ions. The oxidant/fuel ratio of the system was adjusted by adding sufficient quantity of concentrated nitric acid. Amount of citric acid was calculated based on total valence of the

oxidizing and reducing agents for maximum release of energy during combustion. The resulting translucent solution was heated on a hot plate until it turned into a viscous solution. The solution boils upon heating and undergoes dehydration accompanied by foam. On heating further, the foam get ignites itself due to persistent heating resulting to a voluminous and fluffy product of combustion. The combustion product was subsequently characterized as single phase nanocrystals of $\text{NdBa}_2\text{NbO}_6$. The powder obtained after combustion was annealed at 600°C for half an hour to eliminate any trace of organic impurity that may present in the sample.

2.2 Characterization

Structure of the as-prepared powder was examined by powder X-ray diffraction (XRD) technique using an X-ray Diffractometer (Model Philips XPERT-PRO) with Nickel filtered CuK_α radiation. The Infrared (IR) spectra of the samples were recorded in the range $400\text{-}4000\text{cm}^{-1}$ on a Thermo-Nicolet Avatar 370 Fourier Transform Infrared (FTIR) Spectrometer using KBr pellet method. The Fourier transform Raman spectrum of the nanocrystalline $\text{NdBa}_2\text{NbO}_6$ was recorded at room temperature in the wave number ranging $50\text{-}1200\text{cm}^{-1}$ using Bruker RFS/100S spectrometer at a power level of 150mW and resolution 4cm^{-1} . The samples were excited with Nd:YAG laser lasing at 1064nm and the scattered radiation were detected using Ge detector. Particulate properties of the combustion product were examined using transmission electron microscopy (Model:Hitachi H-600 Japan) operating at 200kV . The samples for Transmission Electron Microscope (TEM) were prepared by ultrasonically dispersing the powder in methanol and allowing a drop of this to dry on a carbon-coated copper grid. The differential thermal analysis (DTA) and thermo gravimetric analyses (TGA) were carried out using Perkin-Elmer TG/DT thermal analyzer in the range $30\text{-}1000^\circ\text{C}$ at a heating rate of $10^\circ\text{C}/\text{min}$. in nitrogen atmosphere. The photoluminescence spectra of the samples were recorded using Perkin Elmer LS-45 luminescence spectrometer. The photons from the source were filtered by an emission spectrometer and fed to a photomultiplier detector. The UV-diffuse reflectance of $\text{NdBa}_2\text{NbO}_6$ was analyzed using Jasco V-570 UV-Vis NIR spectrophotometer.

To study the sinterability of the nanoparticles obtained by the present combustion method, the as-prepared $\text{NdBa}_2\text{NbO}_6$ nanoparticles were mixed with 5% polyvinyl alcohol and pressed in the form of cylindrical pellet of diameter 10mm and thickness $\sim 2\text{mm}$ at a pressure about 350MPa using a hydraulic press. The pellet was then sintered at 1325°C for 2h. The theoretical densities of the $\text{NdBa}_2\text{NbO}_6$ were calculated from the lattice constants and sintered density was calculated following the Archimedes method. The surface morphology of the sintered samples was examined using scanning electron microscopy (SEM, Model- JEOL JSM 6390 LV). For low frequency dielectric studies, the pellets were made in the form of a disc capacitor with the specimen as the dielectric medium. Both the flat surfaces of the sintered pellet were polished and then electroded by applying silver paste. The capacitance of the sample was measured using an LCR meter (Hioki-3532-50 LCR HiTester) in the frequency range $100\text{Hz} - 5\text{MHz}$ at room temperature.

3. Results and discussion

3.1 X-ray diffraction (XRD)

Fig. 1 shows the XRD pattern of the as prepared powder annealed at 600°C for 30 min. All the

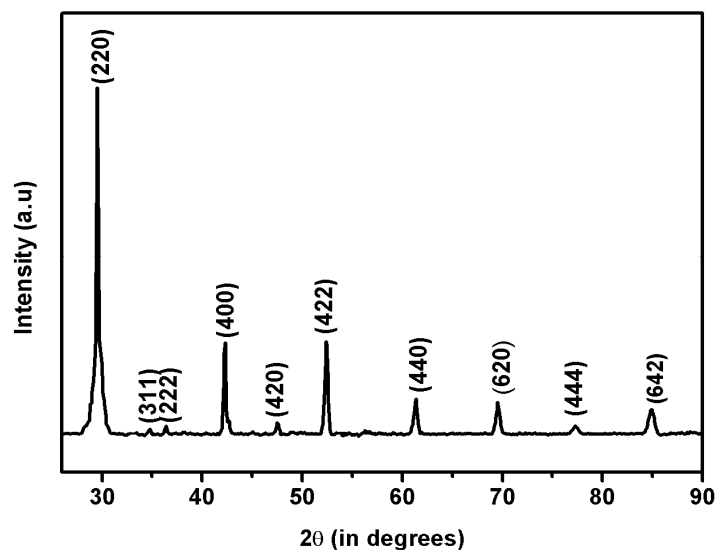


Fig. 1 XRD patterns of nanocrystalline $\text{NdBa}_2\text{NbO}_6$ annealed at 600°C

peaks in the XRD spectrum including the minor one are indexed for the cubic structure ($Fm\bar{3}m$) and the value of lattice parameter calculated from the XRD pattern is 8.340\AA which agree well with the reported standard value (JCPDS 47-0376). The average crystallite size of the combustion product calculated from full-width-half-maximum (FWHM) using Scherrer formula for all the peaks of Fig. 1 is $\sim 35\text{nm}$. This indicates that the phase formation was complete during the combustion synthesis itself.

It may be noted that a single phase $\text{NdBa}_2\text{NbO}_6$ could be obtained through solid state reaction route only after prolonged calcination of the reaction mixture at 1150°C for many hours with multiple intermediate grindings (Kurian *et al.* 1998). In the combustion process reported by Chinarro *et al.* 2007, for the preparation of nanocrystals of ceramic oxides (James *et al.* 2004, Zhang *et al.* 2009) EDTA, polyvinyl alcohol etc. were used as complexing agent and urea as fuels (Chinarro *et al.* 2007, Deganello *et al.* 2009). In these cases, prolonged calcinations of the as-prepared powder at high temperatures were required to obtain a phase pure sample. In the present auto ignition combustion method which uses citric acid as complexing agent and urea as fuel, we were able to prepare phase pure nanopowders of $\text{NdBa}_2\text{NbO}_6$ without any high temperature calcination step. Also we have used niobium pentachloride as a starting material for the synthesis of $\text{NdBa}_2\text{NbO}_6$ which is soluble in hot oxalic acid. The current method offers an easy and time saving method for the preparation of high quality nanopowders of $\text{NdBa}_2\text{NbO}_6$.

3.2 FT-Raman and FTIR analysis

In addition to the powder diffraction studies, we have also recorded the vibrational spectra of the samples for detailed investigation of the structure of the compound. The recorded Raman and IR spectra of $\text{NdBa}_2\text{NbO}_6$ annealed at 600°C are shown in Figs. 2 and 3 respectively.

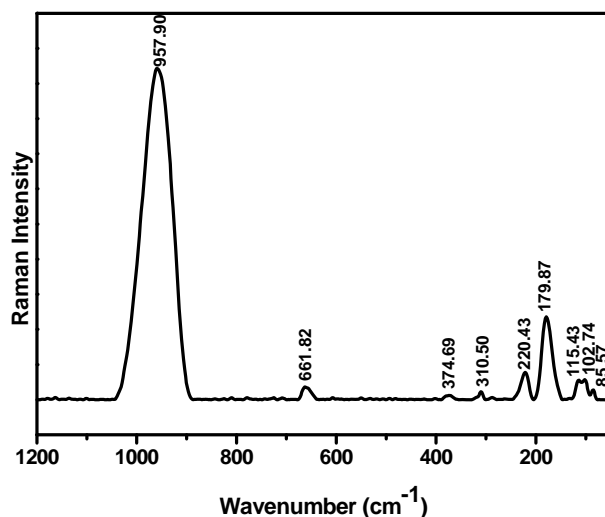


Fig. 2 FT- Raman spectrum of nano NdBa₂NbO₆ annealed at 600°C

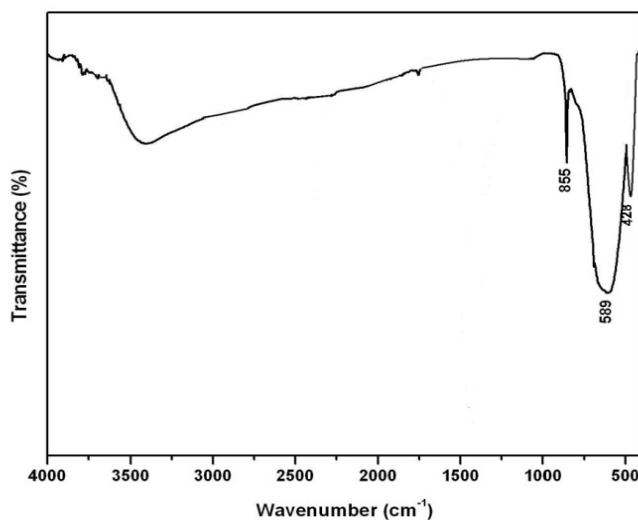


Fig. 3 FT-IR spectra of nano NdBa₂NbO₆ annealed at 600°C

The compound of NdBa₂NbO₆ is a complex perovskite ceramic material, belonging to the family of A₂BB'O₆. The X-ray diffraction study reveals that the compound has a cubic structure with Fm $\bar{3}$ m symmetry. The group theoretical analysis using the standard correlation method predicts 27 normal modes which are distributed as (Vijayakumar *et al.* 2009, Ratheesh *et al.* 2000).

$$\Gamma = A_{1g}(R) + E_g(R) + F_{1g}(\text{silent}) + 2F_{2g}(R) + 4 F_{1u}(\text{IR}) + F_{2u}(\text{silent})$$

According to the group theoretical analysis, the complex perovskite A₂BB'O₆ with a cubic space group Fm $\bar{3}$ m has only four Raman active modes. The four Raman active modes A_{1g}, E_g and

$2F_{2g}$ are observed as strong bands at 956, 662, 374 cm^{-1} and 135–84 cm^{-1} respectively (Ratheesh *et al.* 2000, Rout *et al.* 2008). The A_{1g} mode due to the symmetric stretching vibration of NbO_6 octahedron, when all the cations are at rest and oxygen atom alone moves along the B–O–B' axis, in the highest frequency band while the E_g mode of vibration due to the antisymmetric vibration of the octahedron. The F_{2g} modes characterized by the allowed transition of large A cation are observed at the lower wave numbers. The F_{2g} mode of vibration due to the symmetric bending of the octahedron contributes the medium band at 374 cm^{-1} (Ratheesh *et al.* 2000, Rout *et al.* 2008). The $F_{2g}(1)$ mode of vibration, the position of which is related to the cell parameters irrespective of the chemical nature of the B cation, shows a doublet structure with component at 115 and 102 cm^{-1} .

In the FT-IR spectra shown in Fig. 3 all the peaks are characteristics of the material except at 3416 cm^{-1} which is attributed to the stretching mode of O-H bond due to the presence of adsorbed moisture. Of the four IR active modes, the A_{1g} mode is assigned to the intense band at 855 cm^{-1} . The F_{1u} modes is observed as a highly intense absorption band at 589 cm^{-1} and the $F_{1u}(2)$ mode is observed at 428 cm^{-1} . These modes have become active in the Raman spectrum and are observed as less intense bands in the corresponding regions, indicating a lower symmetry for crystal.

The other two F_{1u} modes are also active in the Raman spectrum and show multiplet structure. The $F_{1u}(3)$ mode is observed at 310 and 288 cm^{-1} and $F_{1u}(4)$ mode at 220 and 179 cm^{-1} . The tilted and distorted octahedral in the compound thereby causing multiplicity and also the IR active F_{1u} modes and the inactive F_{2u} mode have become active in the Raman spectrum.

3.3 Thermal analysis (DTA-TGA)

In order to estimate the loss of weight during annealing the thermo-gravimetric and differential thermal analysis of nanopowders of $\text{NdBa}_2\text{NbO}_6$ were carried out. Fig. 4 shows the DTA-TGA curves of as prepared $\text{NdBa}_2\text{NbO}_6$ obtained directly after combustion. A small weight loss of about 1% was observed in the TGA curve at about 100°C which is due to the liberation of adsorbed moisture present in the sample due to the ultra-fine nature of the as prepared nano powder. A small weight loss of greater than 1% was observed in the TGA curve in the range 550°C, which is due to decomposition of traces of organic impurities which may remained in the

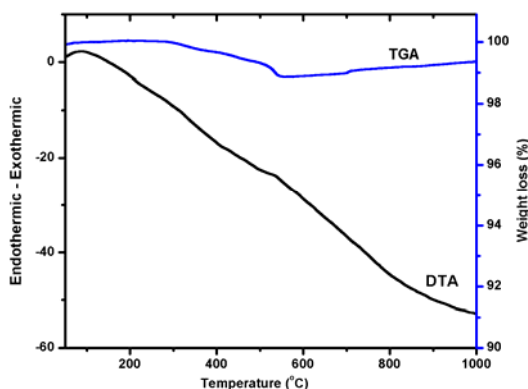


Fig. 4 DTA-TGA curves of as-prepared nanocrystalline $\text{NdBa}_2\text{NbO}_6$

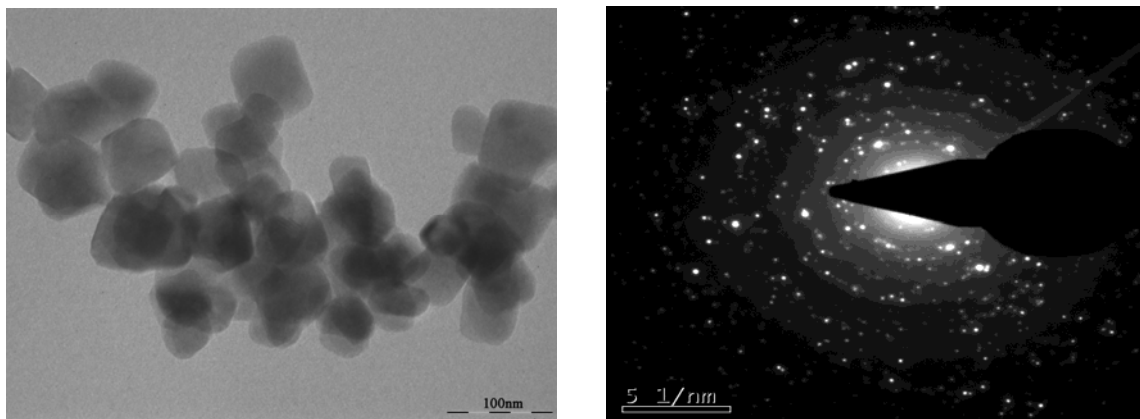


Fig. 5(a) TEM Images of 600°C heated $\text{NdBa}_2\text{NbO}_6$ Fig. 5(b) SAED pattern of 600°C heated $\text{NdBa}_2\text{NbO}_6$

as prepared powder after the combustion. There after no considerable weight change was observed on the TGA curve. The endothermic changes observed in the DTA curve can be attributed to elimination of adsorbed moisture on the sample surface. No evidences of any phase transition taking place in the sample up to this temperature was observed. The variation in DTA curves is in good agreement with the observations in the TGA curve which implies that the phase formation is complete during the combustion itself and there is no further calcinations step required as in the case of conventional solid state route of preparations for phase formation.

3.4 TEM analysis

Fig. 5(a) shows the typical TEM morphologies of the $\text{NdBa}_2\text{NbO}_6$ nanopowder annealed at 600°C for 30min. It is seen that the nanoparticles are of submicron size. The average grain size is about 37 nm. The particles are little agglomerated. The particles are of regular cuboidal shape with sharp grain boundaries. Individual crystallites in the agglomerates appear well bonded with very few voids in between. The corresponding selected area electron diffraction pattern is also showed in the Fig. 5(b). The ring nature of the is indicative of the poly crystalline nature of the crystallites, but the spotty nature of the SAD pattern can be due to the fact that the finer crystallites having related orientations are agglomerated together resulting in a limited set of orientations.

3.5 Photoluminescence study

Photoluminescence is typically performed to investigate the optical properties of quantum confined systems. In order to study the optical property of the prepared sample the photoluminescent activity of the sample is investigated by recording the PL emission spectra of the sample annealed at 600°C. The photoluminescent spectra obtained at the excitation wavelength 350 nm of the sample is given in Fig. 6. The sample exhibits good luminescent property in the visible region. The material shows emission peak in blue, blue-green and green region. The transmission responsible for each emission is identified on the basis of the data by Payling and Larkins (Payling and Larkins 2000). The intense peak at 438 nm in the blue region corresponds to $4f_4[5I]6s4l_{1.5} \rightarrow 0 A_{3.5}^0$ of Nd^{III} . The peak 482.7 nm in the blue-green corresponds to $4f_4[5I]6s4l_{1.5} \rightarrow$

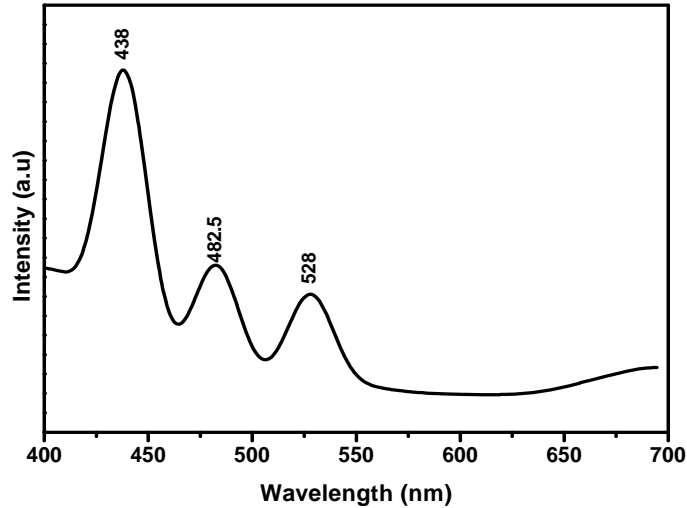


Fig. 6 PL emission spectrum of nanocrystalline $\text{NdBa}_2\text{NbO}_6$

$0 A_{3,5}^0$ of Nd_{II} . The broad peak at 528nm in the green region is attributed to $4F_{1,5}^1 \rightarrow 4D_{0,5}^0$ transition of Nb_I .

Wide-band gap compounds are especially promising for light emitting devices in the short wavelength region of the visible light. Fig. 7(a) and 7(b) depicts the absorbance and reflectance spectrum of the $\text{NdBa}_2\text{NbO}_6$ sample. The absorption spectrum of $\text{NdBa}_2\text{NbO}_6$ exhibits typical optical behavior of a wide-band gap semiconducting compound, having an intense absorption band around 266 nm with a steep edge. From the absorption spectra it is clear that the sample absorbs heavily within the UV – region. It reveals that $\text{NdBa}_2\text{NbO}_6$ nanomaterials can readily respond to ultraviolet. Such materials find application in filters and sensors for UV– radiation.

3.6 UV- Vis. analysis (DRS)

Diffuse reflectance spectroscopy (DRS) is a simple but powerful spectroscopic technique to determine the band gap energy (E_g) of powder samples unambiguously. The estimation of band gap energy using DR spectra was proposed by Kubelka and Munk; the measured reflectance (R) being expressed as $k/s = (1-R)^2/2R$ where k is the absorption coefficient and s is the scattering coefficient (Barton *et al.* 1999, Aneesh *et al.* 2009).

The band gap energy was determined by extrapolating the UV-DRS spectrum as shown in Fig. 7(c) by plotting $h\nu$ and $[k/s \times h\nu]^2$ where k is the absorption co-efficient and s is the scattering coefficient. The band gap (E_g) of the material is estimated by extrapolating the straight line in the graph at $k=0$. The value of band gap obtained is 3.9 eV. This corresponds to ultraviolet (UV) radiation for optical inter-banded transitions with a wavelength 370 nm. The obtained 3.9 eV is in the wide-band gap semiconductor compound which has broad range of applications including light emitting devices, varistors, solar cell and gas sensors. Zhang *et al.* reported that a blue-shift occurs when particle size reduces (Zhang *et al.* 2009).

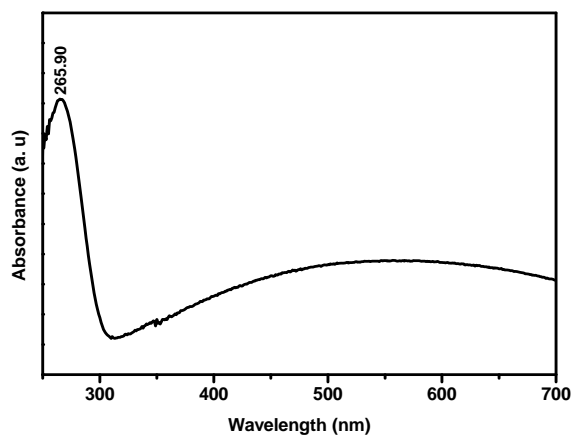


Fig. 7(a) Absorbance spectrum of nanocrystalline NdBa₂NbO₆

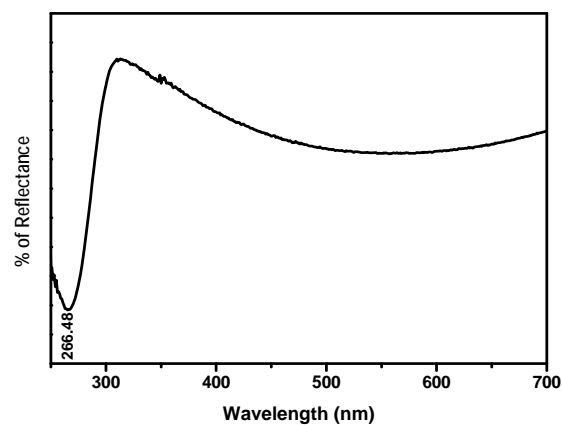


Fig. 7(b) Reflectance spectrum of nanocrystalline NdBa₂NbO₆

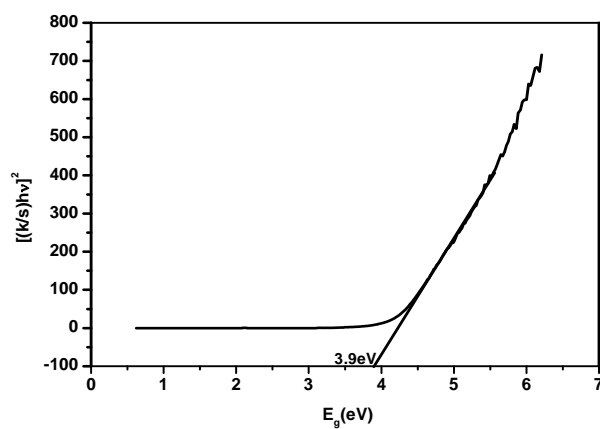


Fig. 7(c) $h\nu - [(k/s)h\nu]^2$ graph of the nanocrystalline NdBa₂NbO₆

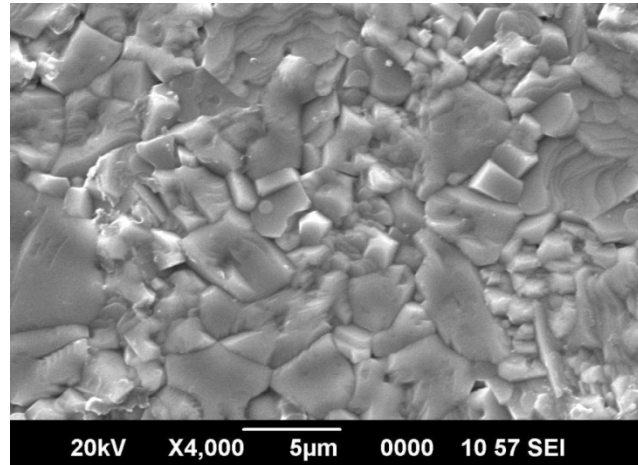


Fig. 8 SEM images of $\text{NdBa}_2\text{NbO}_6$

3.7 Sintering behavior and SEM analysis

For microwave dielectric and electronic device applications it is necessary to specify some minimum value of dielectric constant that must lie between 35 and 55. Hence it is important to study the sintering behavior of the sample. The sintering behavior of the nanocrystals of $\text{NdBa}_2\text{NbO}_6$ powders synthesized through the present combustion route was studied in detail at different trials. The relative green density of the specimen used for the sintering study was $\sim 55\%$. An optimum and best value of sintered density of about 96% of the theoretical density was obtained on sintering the compacted specimen at 1325°C for 2h. Generally micron sized $\text{NdBa}_2\text{NbO}_6$ powder requires very high sintering temperature $1575\text{-}1600^\circ\text{C}$ for many hours without any sintering aid for better densification (Dias *et al.* 2006, Koshy *et al.* 1994). The high sintered density of the compacted nanopowder and the reduced temperature-time schedule can be attributed to the enhanced kinetics due to the small degree of agglomeration, its grain morphology and ultra-fine nature of $\text{NdBa}_2\text{NbO}_6$ prepared by the present method of synthesis.

It is clear from the SEM micrographs shown in Fig. 8 that densification was achieved without significant microstructural coarsening. Moreover no cracks or pores were observed on the surface. Microstructure reveals an increase in grain growth and associated orientation with sintering temperature.

3.8 Dielectric properties

The dielectric behavior of sintered samples of $\text{NdBa}_2\text{NbO}_6$ nanocrystals is shown in Fig. 9. Here the variation of dielectric constant with frequency is observed with that reported earlier ($\epsilon_r = 38$) for pellets prepared from micron-sized particles (Kurian *et al.* 1998). For the present study the dielectric constant and loss tangent ($\tan\delta$) for 5 MHz are about 43 and 1.97×10^{-4} respectively. For higher selectivity and optimizing bandwidth filter designers prefer to use complex isostructural perovskites compounds (Dias *et al.* 2006). The high demand and increased price for tantalum based complex perovskite compounds have diverted attention to a new composition based on isostructural perovskite niobium compound. In the present study the values of dielectric

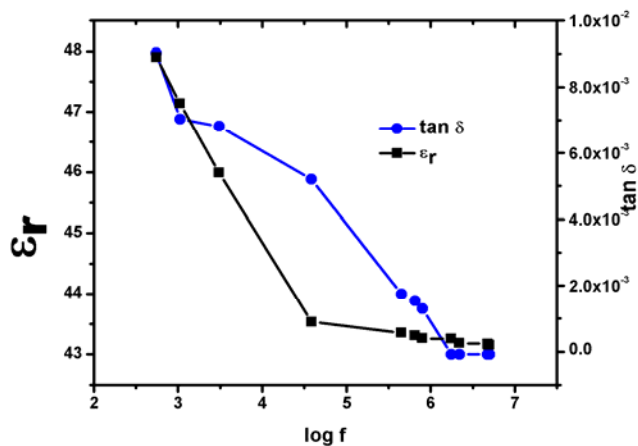


Fig. 9 Dielectric response of $\text{NdBa}_2\text{NbO}_6$ with frequency

parameters were observed as $\epsilon_r = 43$ and loss factor $\tan \delta = 1.97 \times 10^{-4}$ at 5 MHz. The enhanced ϵ_r in the present study may also be due to the fine grain growth and associated orientation. Hence it is a promising material for moderately high ϵ_r value dielectric material.

4. Conclusions

Nanoparticles of $\text{NdBa}_2\text{NbO}_6$ have been synthesized using a modified combustion method for the first time. In the present modified combustion method no calcinations step was needed to obtain phase pure powder of $\text{NdBa}_2\text{NbO}_6$. The studies reveal that the nano powder is single phase with distorted cubic structure with lattice constant 8.340 Å. Average particle size from TEM image is 37nm. The TGA and DTA curves show the sample is thermally stable with no phase transition. Photo luminescent spectra of the sample show intense emission peaks in the visible region. The average optical band gap determined from UV–vis absorption spectra is 3.9 eV which indicates the sample is a semiconductor. These nanocrystals could be sintered at a temperature of 1325°C to a density of about 96%. The SEM image of the sintered material indicates high densification of the material. The room-temperature dielectric constant (ϵ_r) and loss factor of the sintered pellet at 5MHz was 43 and 1.97×10^{-4} respectively. The decrease in sintering temperature compared to conventional sample, high dielectric constant and low loss makes $\text{NdBa}_2\text{NbO}_6$ an excellent candidate for dielectric applications.

References

- An, C.H., Tang, K.B., Wang, C.R., Shen, G.Z., Jin, Y. and Qian, Y.T. (2002), "Characterization of LiNbO_3 nanocrystals prepared via a convenient hydrothermal route", *Mater. Res. Bull.*, **37**(11), 1791-1796.
- Aneesh, P.M., Mini, K.K. and Jayaraj, M.K. (2009), "Hydrothermal synthesis and characterization of undoped and Eu doped ZnGa_2O_4 nanoparticles", *J. Electrochem. Soc.*, **156**(3), K33-K36.

- Aruna, S.T. and Mukasyan, A.S. (2008), "Combustion synthesis and nanomaterials", *Cur. Opin. Solid. St. Mater.*, **12**, 44-50.
- Aven, M. and Prener, J.S. (1967), *Physics and Chemistry of II-VI Compounds*, North Holland, Amsterdam.
- Bhalla, A.S., Guo, R.Y. and Roy, R. (2000), "The perovskite structure - a review of its role in ceramic science and technology", *Mater. Res. Innov.*, **4**(1), 3-26.
- Chinarro, E., Jurado, J.R. and Colomer, M.T. (2007), "Synthesis of ceria-based electrolyte, nanometric powders by urea-combustion technique", *J. Eur. Ceram. Soc.*, **27**(13-15), 3619-3623.
- Cruickshank, D. (2003), "1-2 GHz dielectrics and ferrites: overview and perspectives", *J. Eur. Ceram. Soc.*, **23**(14), 2721-2726.
- Barton, D.G., Shtein, M., Wilson, R.D., Soled, S.L. and Iglesia, E. (1999), "Structure and electronics properties of solid acids based on tungsten oxide nanostructures", *J. Phys. Chem.*, **103**(4) 630-640.
- Deganello, F., Marci, G. and Deganello, G. (2009), "Citrate-nitrate auto-combustion synthesis of perovskite-type nanopowders: A systematic approach", *J. Eur. Ceram. Soc.*, **29**(3), 439-450.
- Denzler, D., Olschewski, M. and Sattler, K. (1998), "Luminescence studies of localized gap states in colloidal ZnS nanocrystals", *J. Appl. Phys.*, **84**(5), 2841-2845.
- Dias, A., Abdulkalam, L., Sebastian, T.M., Paschol, C.W.A. and Moreira, L.R. (2006), "Chemical substitution in Ba (RE1/2Nb1/2)O-3 (RE = La, Nd, Sm, Gd, Tb, and Y) microwave ceramics and its influence on the crystal structure and phonon modes", *Chem. Mater.*, **18**, 214 -220.
- Gleiter, H. (2000), "Nanostructured materials: basic concepts and microstructure", *Acta Mater.*, **48**(1), 1-29.
- Goldberg, P. (1966), *Luminescence of Inorganic Solids*, Academic Press, New York.
- Gruber, D., Kraus, F. and Muller, J. (2003), "A novel gas sensor design based on $\text{CH}_4/\text{H}_2/\text{H}_2\text{O}$ plasma etched ZnO thin films", *Sensor. Actuat. B Chem.*, **92**(1-2), 81-89.
- Guo, Y.P., Kakimoto, K. and Ohsato, H. (2004), "Phase transitional behavior and piezoelectric properties of $(\text{Na}_{0.5}\text{K}_{0.5})\text{NbO}_3\text{-LiNbO}_3$ ceramics", *Appl. Phys. Lett.*, **85**(18), 4121-4123.
- Henglein, A. (1989), "Small-particle research: physicochemical properties of extremely small colloidal metal and semiconductor particles", *Che. Rev.*, **89**(8), 1861-1873.
- Huang, M.H., Mao, S., Feick, H., Yan, H., Wu, Y., Kind, H., Weber, E., Russo, R. and Yang, P. (2001), "Room-temperature ultraviolet nanowire nanolasers", *Science* **292**(5523), 1897-1899.
- Hughes, H., Iddles, D.M. and Reaney, I.M. (2001), "Niobate-based microwave dielectrics suitable for third generation mobile phone base stations", *Appl. Phys. Lett.*, **79**(18), 2952-2954.
- James, J., Jose, R., John, A.M. and Koshy, J. (2004), "Single Step process for the synthesis of nanoparticles of ceramic oxide powders", US Patent No 6, 835, 367.
- Kurian, J., John, A.M., Sajith, P.K., Koshy, J., Pai, S.P. and Pinto, R. (1998), "Superconducting $\text{YBa}_2\text{Cu}_3\text{O}_{7-\delta}$ -Ag Thin films ($T_c(0) = 90$ K) by pulses Laser Deposition on Polycrystalline $\text{Ba}_2\text{NdNbO}_6$: A novel substrate for $\text{YBa}_2\text{Cu}_3\text{O}_{7-\delta}$ -Ag films", *Jpn. J. Appl. Phys.*, **37**(10A), L1114-L1117.
- Jose, R., James, J., John, A.M., Divakar, R. and Koshy, J. (2000), "Synthesis of nanosized $\text{Ba}_2\text{LaZrO}_{5.5}$ ceramic powders through a novel combustion route", *J. Mater. Synth. Process*, **8**(1), 1-5.
- Keis, K., Magnusson, E., Lindstrom, H., Lindquist, S.E., and Hagfeldt, A. (2002), "A 5% efficient photoelectrochemical solar cell based on nanostructured ZnO electrodes", *Sol. Energy Mater. Sol. Cells*, **73**(1), 51-58.
- Kong, L.B., Zhang, T.S., Ma, J. and Boey, F. (2008), "Progress in synthesis of ferroelectric ceramic materials via high-energy mechanochemical technique", *Prog. Mater.Sci.*, **53**(2), 207-322.
- Koshy, J., Kurian, J., Thomas, J.K., Yadava, Y.P. and Dhamodaran, A.D. (1994), "Rare earth Barium niobates a new class of potential substrates for YBCO superconductor", *Jpn. J. Appl. Phys.*, **33**, 117-121.
- Koshy, J., Kumar, K.S., Kurian, J., Yadava, Y.P. and Damodaran, A.D. (1994), " $\text{YBa}_2\text{SnO}_{5.5}$, a novel ceramic substrate for YBCO and BiSCCO superconductors", *Bull. Mater. Sci.*, **17**(6), 577-584.
- Koshy, J., Thomas, J.K., Kurian, J., Yadava, Y.P. and Damodaran, A.D. (1993), " $\text{GdBa}_2\text{NbO}_6$ a new ceramic substrate for YBCO thick films", *Mater. Lett.*, **17**(6), 393-397.
- Kurian, J., Nair, K.V.O., Sajith, P.K., John, A.N. and Koshy, J., (1998), "Bi(2223) thick films ($T_c(0) = 109\text{K}$) on $\text{Ba}_2\text{GdNbO}_6$ a new perovskite ceramic substrate for BSCCO superconductor", *Appl. Supercond.*, **6**(6), 301-304.

- Magrez, A., Vasco, E., Seo, J.W., Dieker, C., Setter, N. and Forro, L. (2006), "Growth of single crystalline KNbO₃ nanostructures", *J. Phys. Chem. B*, **110**(1), 58-61.
- Mahan, G.D. (1983), "Intrinsic defects in ZnO varistors", *J. Appl. Phys.*, **54**(7), 3825-3832.
- Matthias, B.T., and Remeika, J.P. (1949), "Ferroelectricity in the Ilmenite Structure", *Phys.Rev.*, **76**(12), 1886-1887.
- Zhang, M., Hue, C., Liu, H., Xiong, Y.F. and Zhang, Z. (2009), "A rapid - response humidity sensor based on BaNbO₃ crystals", *Sensor. Actuat. B Chem.*, **136**(1), 128-132.
- Niederberger, M., Pinna, N., Polleux, J. and Antonietti, M. (2004), "A general soft-chemistry route to perovskites and related materials: Synthesis of BaTiO₃, BaZrO₃, and LiNbO₃ nanoparticles", **43**(17), *Angew. Chem. Int. Edit.*, 2270-2273.
- Padmakumar, H., Vijayakumar, C., George, C.N., Solomon, S., Jose, R., Thomas, J.K. and Koshy, J. (2008), "Characterization and sintering of BaZrO₃ nanoparticles synthesized through a single-step combustion process", *J. Alloy. Compd.*, **458**(1-2), 528-531.
- Patro, P.K., Kulkarni, A.R. and Harendranath, C.S. (2003), "Combustion synthesis of Sr_{0.5}Ba_{0.5}Nb₂O₆ and effect of fuel on its microstructure and dielectric properties", *Mater. Sci. Bull.*, **38**(2), 245-259.
- Payling, R. and Larkins, P. (2000), *Optical Emission Line of Elements*, John Wiley and sons, New York.
- Prasanth, C.S., Padmakumar, H., Pazhani, R., Solomon, S. and Thomas, J.K. (2008), "Synthesis, characterization and microwave dielectric properties of nanocrystalline CaZrO₃ ceramics", *J. Alloy. Compd.*, **464**(1-2), 306-309.
- Ramanujan, R.V., (2003), "Nanostructured electronic and magnetic materials", *Sadhana*, **25**(1-2), 81-96.
- Ratheesh, R., Wo` hlecke, M., Berge, B., Wahlbrink, T., Haeuseler, H., Rul, E., Blachnik, R., Balan, P., Santana, N. and Sebastian, M.T., (2000), "Raman study of the ordering in SrB_{0.5}Nb_{0.5}O₃ compounds", *J. Appl. Phys.*, **88**, 2813-2818.
- Ianoş, R., Lazau, I., Pacurariu, C. and Barvinschi, P. (2009), "Fuel mixture approach for solution combustion synthesis of Ca₃Al₂O₆ powders", *Cement Concrete Res.*, **39**(7), 566-572.
- Rout, D., Babu, G.S., Subramanian, V. and Sivasubramanian, V. (2008), "Study of Cation Ordering in Ba(Yb_{1/2}Ta_{1/2})O₃ by X-Ray Diffraction and Raman Spectroscopy", *Int. J. Appl. Ceram. Technol.*, **5**(5), 522-528.
- Saito, Y., Takao, H., Tani, T., Nonoyama, T., Takatori, K., Homma, T., Nagaya, T. and Nakamura, M. (2004), "Lead-free piezoceramics", *Nature*, **432**(7013), 84-87.
- Schwesyg, J.R., Eggert, H.A., Buse, K., Sliwinska, E., Khalil, S., Kaiser, M. and Meerholz, K. (2007), "Fabrication and optical characterization of stable suspensions of iron- or copper-doped lithium niobate nanocrystals in heptanes", *Appl. Phys. B- Lasers and Optics*, **89**(1), 15-17.
- Specking, W., Kiesel, H., Nakajima, H., Ando, T., Tsuji, H., Yamada, Y. and Nagata, M. (1993), "First results of stress effects on I_c of Nb₃Al cable in conduit fusion superconductors", *IEEE. T. Appl. Supercon.*, **3**(1), 1342-1345.
- Suryanarayana, C. (1994), "Structure and properties of nanocrystalline materials", *Bull. Mater. Sci.*, **17**(4), 307-346.
- Thomas, J.K., Padmakumar, H., Pazhani, R., Solomon, S., Jose, R. and Koshy, J. (2006), "Synthesis of strontium zirconate as nanocrystals through a single step combustion process", *Mater. Lett.*, **61**(7), 1592-1595.
- Vijayakumar, C., Padma Kumar, H., Solomon, S., Thomas, J.K., Wariar, P.R.S. and John, A. (2009), "FT-Raman and FT-IR vibrational spectroscopic studies of nanocrystalline Ba₂RESbO₆ (RE = Sm, Gd, Dy and Y) perovskites", *J. Alloys Compd.*, **480**(2), 167-170.
- Wang, L.H., Yuan, D.R., Duan, X.L., Wang, X.Q. and Yu, F.P. (2007), "Synthesis and characterization of fine lithium niobate powders by sol-gel method", *Crys. Res. Technol.*, **42**(4), 321-324.
- Wang, X., Zhuang, J., Peng, Q. and Li, Y. (2005), "A general strategy for nanocrystal synthesis", *Nature*, **437**, 121-124.
- Wood, B.D., Mocanu, V. and Gates, B.D. (2008), "Solution-phase synthesis of crystalline lithium niobate nanostructures", *Adv. Mater.*, **20**(23), 4552-4556.
- Wooten, E.L., Kissa, K.M., Yi-Yan, A., Murphy, E.J., Lafaw, D.A., Hallemeier, P.F., Maack, D., Attanasio,

- D.V., Fritz, D.J., McBrien, G.J. and Bossi, D.E. (2000), "A review of lithium niobate modulators for fiber-optic communications systems", *IEEE J. Sel. Top. Quant.*, **6**(1), 69-82.
- Zhao, L.L., Steinhart, M., Yosef, M., Lee, S.K. and Schlecht, S. (2005), "Large-scale template-assisted growth of LiNbO_3 one-dimensional nanostructures for nano-sensors", *Sens. Actuat. B-Chem.*, **109**(1), 86-90.
- Zupan, K., Marinšek, M., Pejovnik, S., Maček, J. and Zore, K. (2004), "Combustion synthesis and the influence of precursor packing on the sintering properties of LCC nanopowders", *J. Eur. Ceram. Soc.*, **24**, 1935-1939.

CC